Supporting Information for

Lateral Size Dependent Colloidal Stability of Graphene Oxide in Water: Impacts of Protein Properties and Water Chemistry

Binbin Sun[a], Yinqing Zhang[a], Qing Liu[a], Chaorui Yan[b], Bowen Xiao[a], Jing Yang[a], Menglin Liu[a], Lingyan Zhu[*a]

[a]Key Laboratory of Pollution Processes and Environmental Criteria (Ministry of Education), Tianjin Key Laboratory of Environmental Remediation and Pollution Control, College of Environmental Science and Engineering, Nankai University, Tianjin 300350, P. R. China

[b]College of Land Science and Technology, China Agricultural University, Beijing 100193, PR China

Summary

Number of Pages: 34

Page S2-S8: Table S1- Table S8

Page S9-S30: Figure S1–Figure S25

[*] To whom correspondence should be addressed. E-mail: zhuly@nankai.edu.cn. Phone: +86-22-23500791. Fax: +86-22-23500791.

Table S1. The portions of functional groups in GO characterized by XPS

Sample	C : O (WT%)	C-C/C=C	C-O-C/C-O	C=O	O-C=O
GO-1	1.3806	0.517	0.3817	0.0826	0.015
GO-2	1.4222	0.513	0.3685	0.101	0.01796
GO-3	1.4045	0.5253	0.3554	0.102	0.0172
GO-4	1.3722	0.4787	0.4121	0.0935	0.0155

Table S2. The bulk elemental composition (%) of GO characterized by elemental analyzer

Sample	N	C	H	S	O	C : O
GO-1	0.705	44.13	2.1225	1.728	51.3145	1.15
GO-2	0.745	43.885	1.76	1.3475	52.2625	1.12
GO-3	0.37	43.505	2.4315	0.5075	53.186	1.09
GO-4	0.525	43.525	2.0565	0.8545	53.039	1.09

Table S3. The fast aggregation rate (k_{fast}) and corresponding critical coagulation concentrations of GO with different lateral sizes at pH 6.0 and 25 ℃.

GO type	k_{fast}	CCC (mM NaCl)	k_{fast}	CCC (mM $CaCl_2$)
GO–1	4.192	173.9	4.418	1.56
GO–2	4.895	225.3	4.299	1.58
GO–3	4.376	249.2	4.964	1.58
GO–4	4.576	278.4	4.947	1.56

Table S4. The selected physicochemical properties of BSA and OVA.

Protein	PI	TOC (%)	MW(kDa)	Bulk elemental composition (%)				
				N	C	H	O	S
BSA	5.0	42.9	67	15.31	51.84	8.97	23.88	ND
OVA	4.8	41.6	45	14.48	49.86	8.86	26.80	ND

PI: electrostatic point; TOC: total organic matter measured by a total organic carbon analyzer (TOC-VCSN, Shimadzu, Japan); MW: molecular weight; ND-not detected

Table S5. Adsorbed layer thickness (d) calculated by Ohshima's soft particle theory.

Organics type	λ	ZN	d (nm)	R^2
BSA	5.63	0.86	5.83	0.986
OVA	3.19	1.633	3.22	0.992

Table S6. The corresponding protein concentrations corresponding to the k values of GO nanosheets at three different regimes at pH 6.0 and 25 ℃.

Samples	OVA (mg/L)		
	$k<k_{fast}$	$k=k_{fast}$	$0\leq k<k_{fast}$
GO–1	0–2.5	2.5–100	100–600
GO–2	0–7.5	7.5–100	100–600
GO–3	0–10	10–100	100–600
GO–4	0–25	25–100	100–600

Table S7. The electrophoretic mobility (EPM, $10^{-8}m^2V^{-1}s^{-1}$) and D_h of 500 nm (GO-2) GO nanoparticles (10 mg/L) in the presence of 1 mM NaCl at different pH values (4, 6 and 9) and 25 ℃, the EPM of OVA (600 mg/L) at different pH values (4, 6 and 9), and the aggregation rate (k) of 500 nm (GO-2) GO nanoparticles in the presence of 120 mM NaCl under different pH values without OVA.

pH value	EPM (GO-2)	GO D_h	EPM (OVA)	k
4.0	-3.27±0.12	186 nm	1.38±0.08	1.113±0.08
6.0	-3.38±0.14	179 nm	-1.61±0.22	0.361±0.063
9.0	-3.19±0.11	183 nm	-2.35±0.09	0.075±0.001

Table S8. The OVA concentrations corresponding to aggregation rate (k) of 500 nm (GO-2) GO nanoparticles at three different regimes under three different pH values and 25 ℃.

pH	OVA concentration (mg/L)		
	$k<k_{fast}$	$k=k_{fast}$	$0\leq k<k_{fast}$
4.0	0-1	1-150	150-600
6.0	0-10	10-150	150-600
9.0	0-75	75	75-300

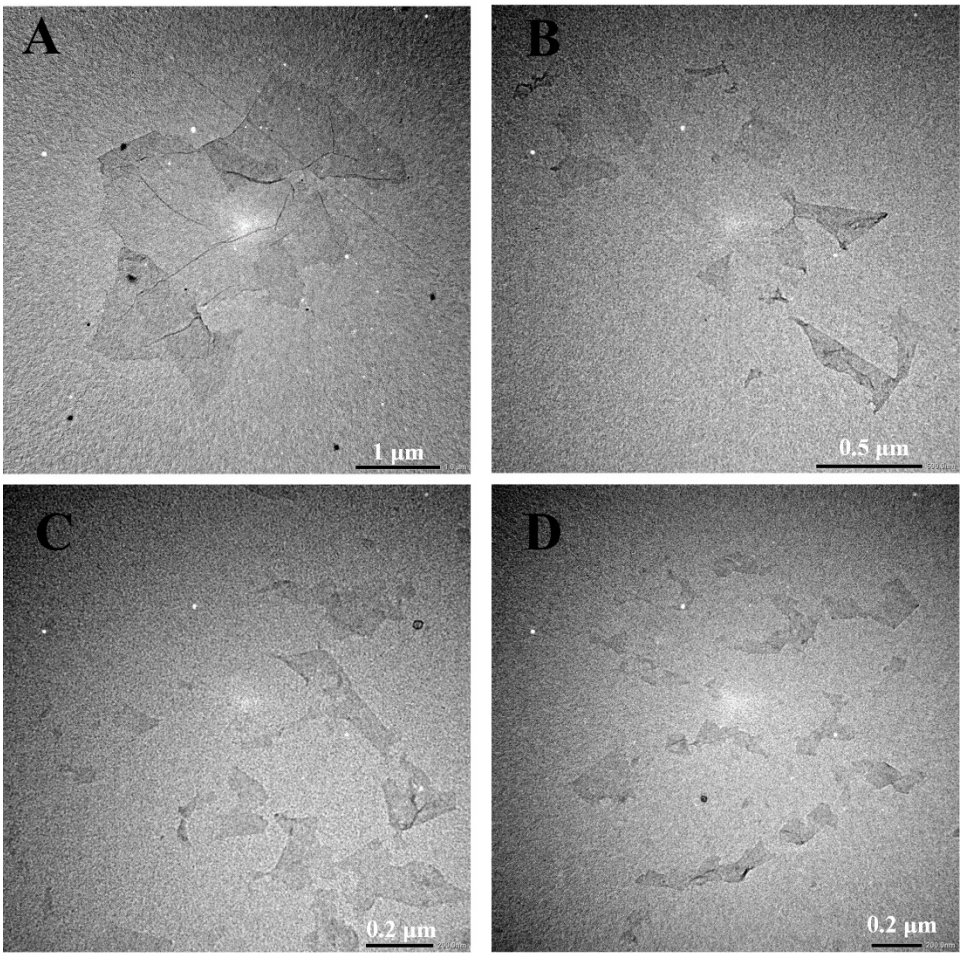

Figure S1. The representative TEM images of GO with different ultrasonication period, 1000 nm (GO-1) (A); 500 nm (GO-2) (B); 350 nm (GO-3) (C) and 200 nm (GO-4) (D) GO nanoparticles.

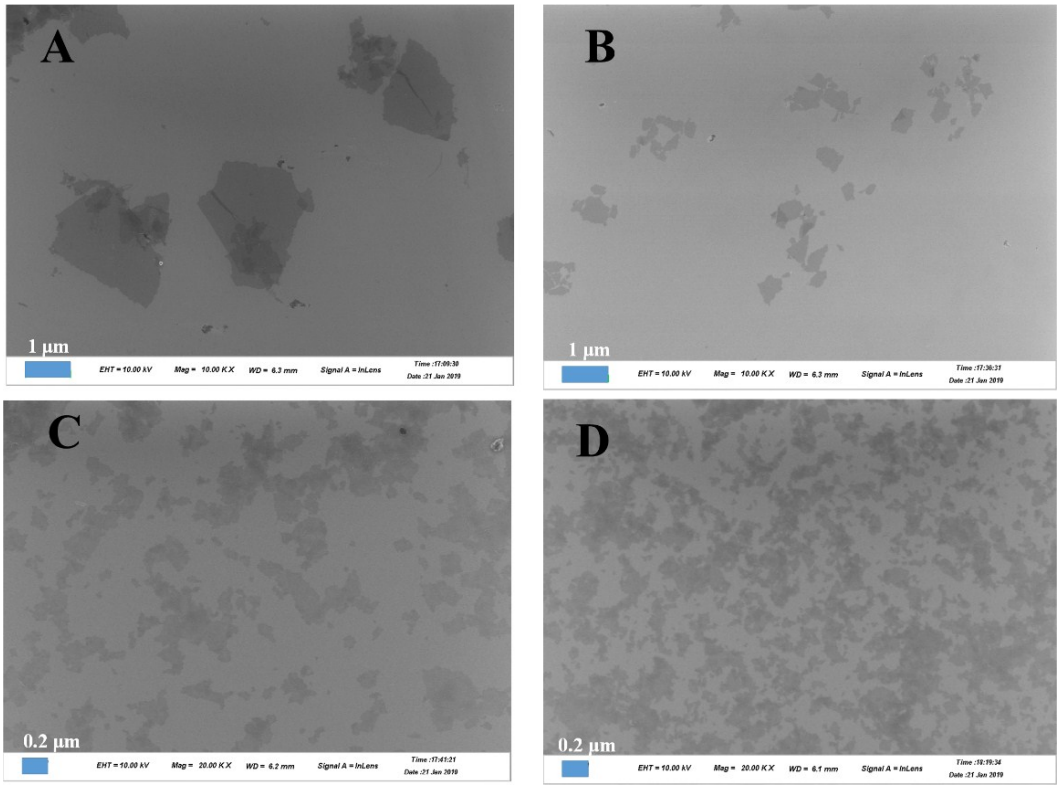

Figure S2. The representative FESEM images of GO with different ultrasonication period, 1000 nm (GO-1) (A); 500 nm (GO-2) (B); 350 nm (GO-3) (C) and 200 nm (GO-4) (D) GO nanoparticles.

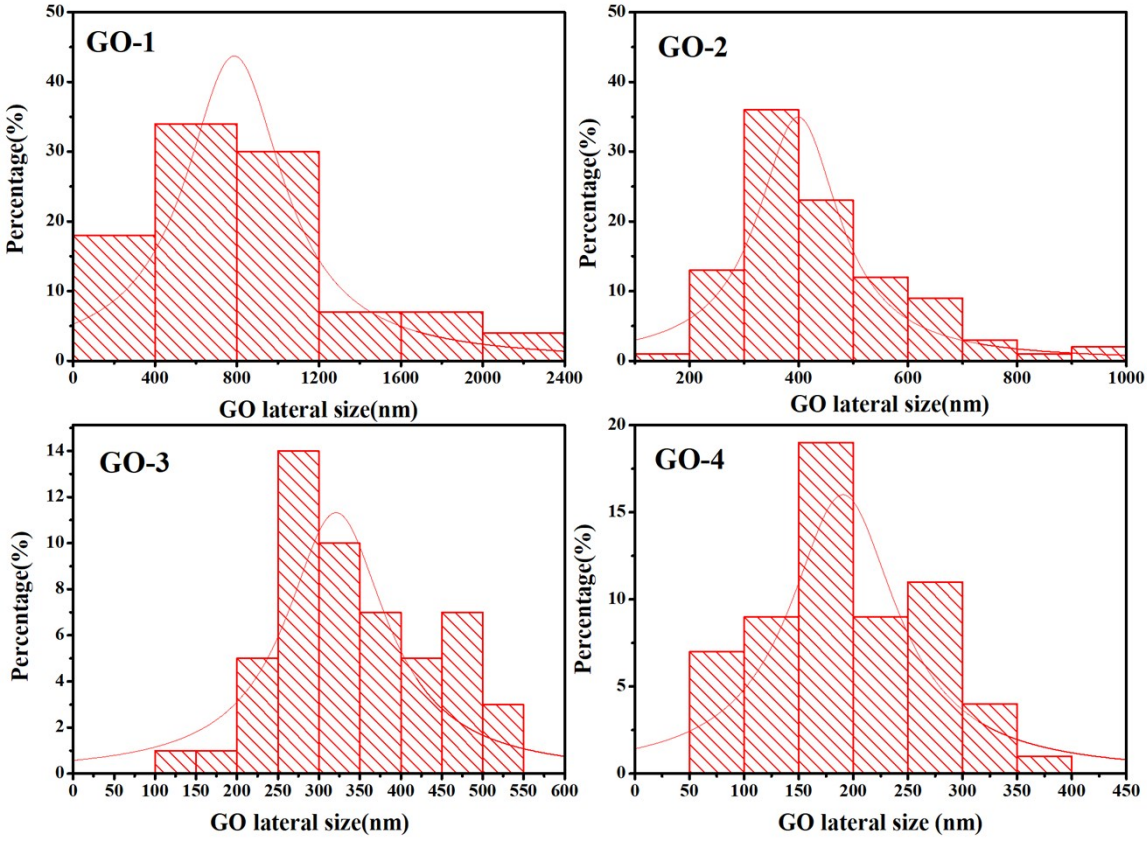

Figure S3. The lateral size distribution of GO samples obtained by at least 150 GO nanosheets from five different FESEM images.

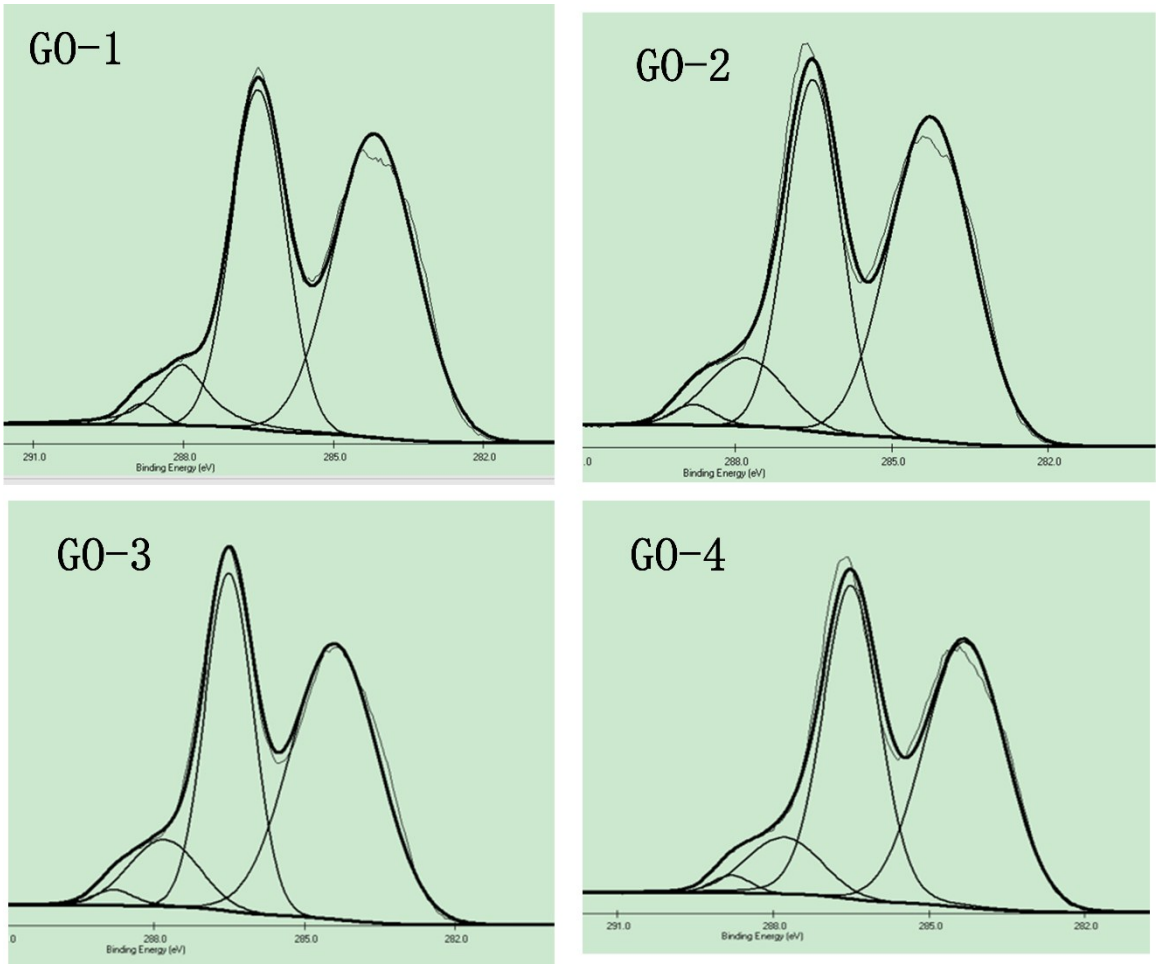

Figure S4. XPS spectra of samples 1000 nm (GO-1) (A), 500 nm (GO-2) (B), 350 nm (GO-3) (C) and 200 nm (GO-4) (D) GO nanoparticles. The peaks with the binding energy of 284.4, 286.5, 287.8 and 288.8 eV are corresponding to the carbon atoms in aromatic rings (C-C/C=C), epoxy/hydroxyl (C-O-C/C-OH), carbonyl (C=O) and carboxyl (O-C=O), respectively.

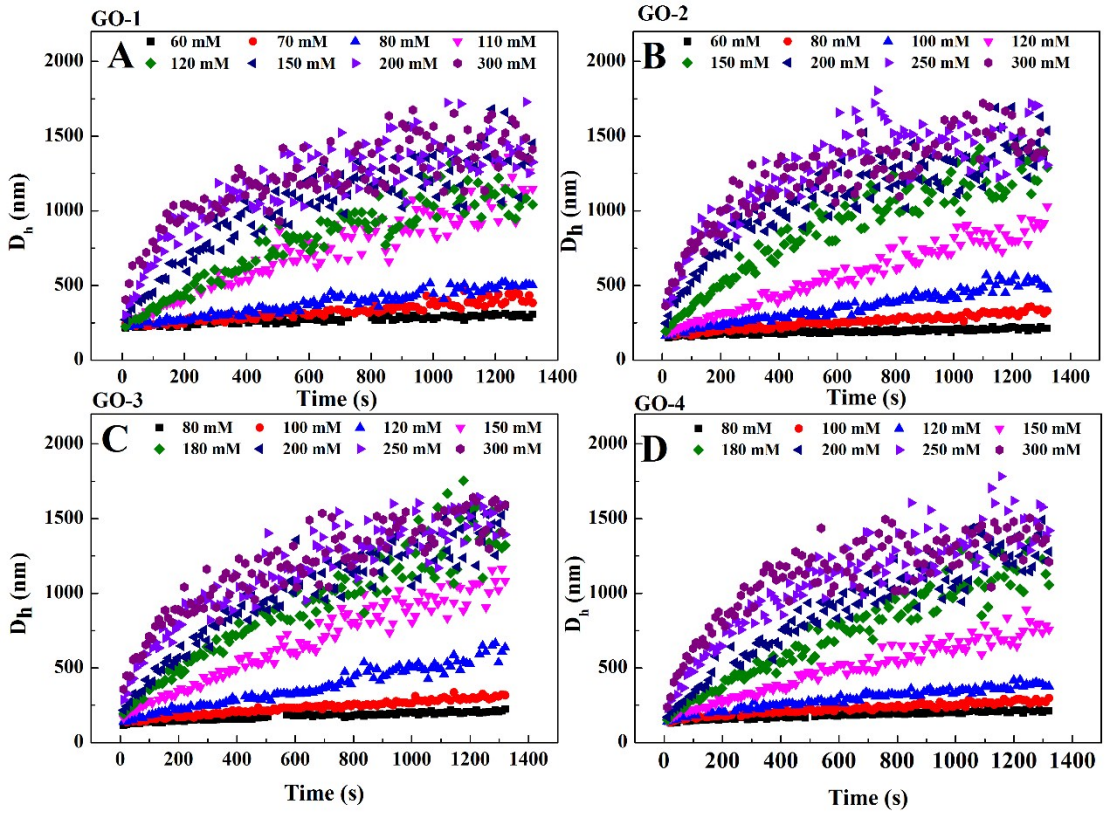

Figure S5. The representative aggregation profiles of GO with four different lateral sizes (1000, 500, 350 and 200 nm) changed as a function of NaCl concentration at pH 6.0 and 25 ℃.

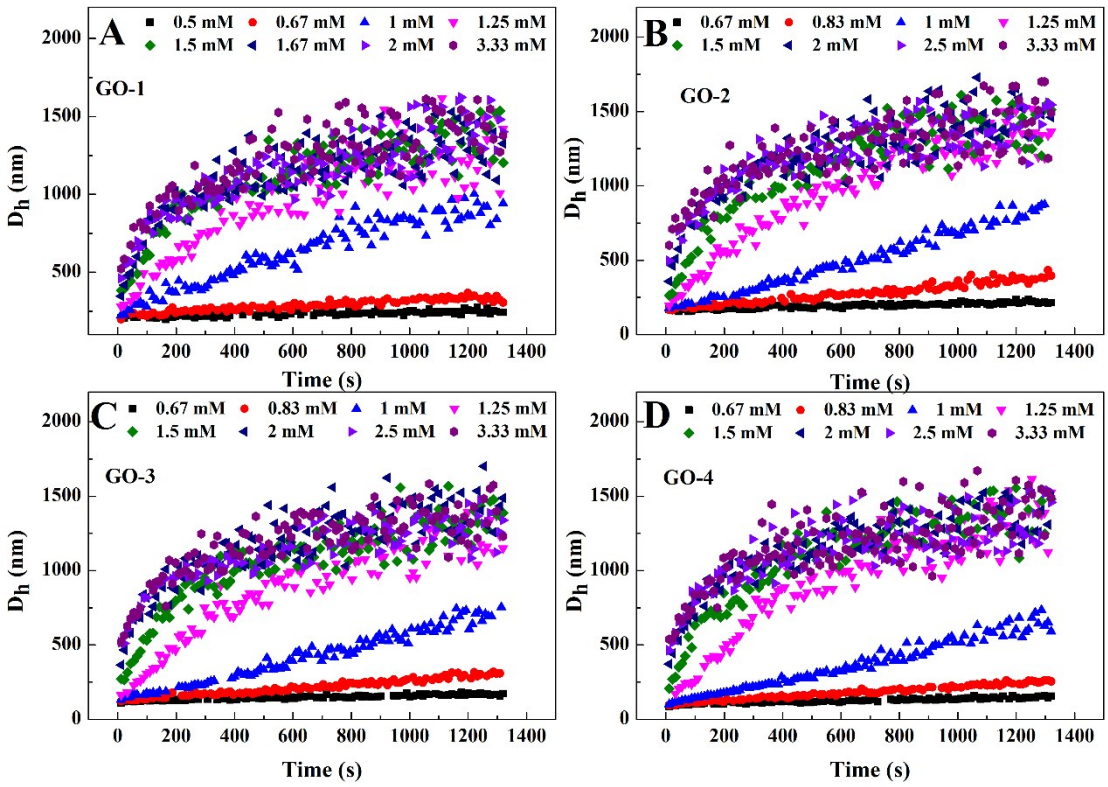

Figure S6. The representative aggregation profiles of GO with four different lateral sizes (1000, 500, 350 and 200 nm) changed as a function of $CaCl_2$ concentration at pH 6.0 and 25 ℃.

A GO-1

B GO-4

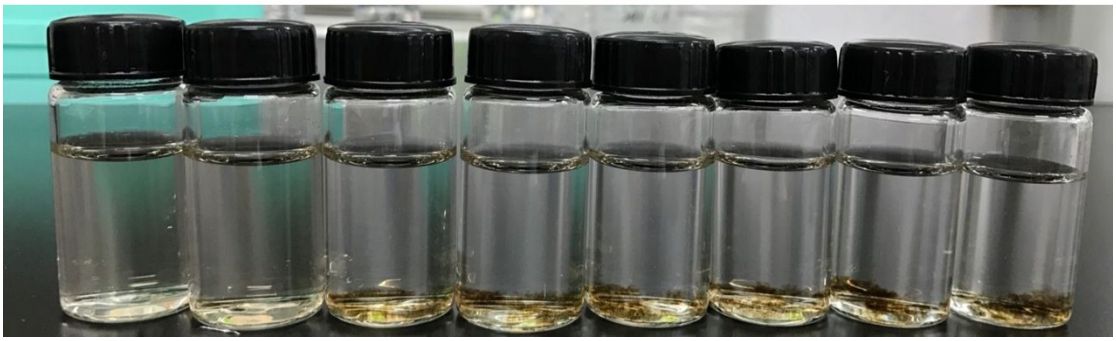

Figure S7. The long-term sedimentation images of 1000 nm (GO-1) (A) and 200 nm (GO-4) (B) GO nanoparticles in the presence of 0, 60, 80, 120, 150, 200, 300 and 600 mM NaCl after 24 h at pH 6.0 and 25 ℃.

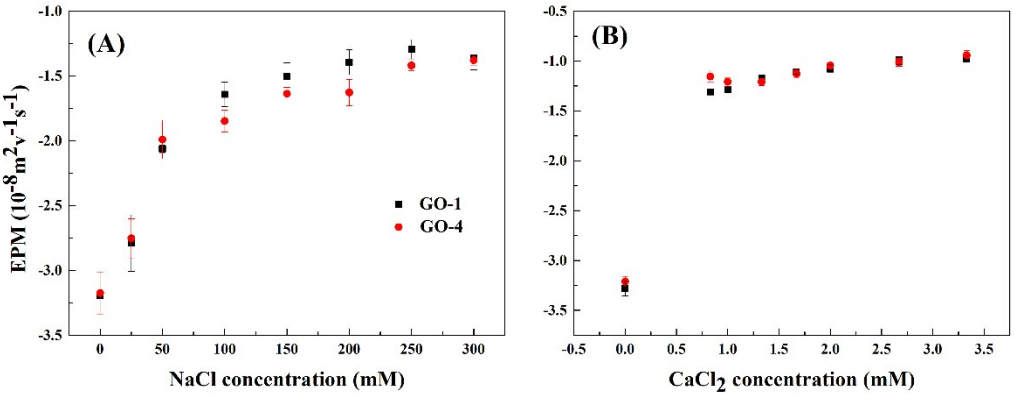

Figure S8. The electrophoretic mobility (EPM) of 1000 nm (GO-1) and 200 nm (GO-4) GO nanoparticles changed as a function of NaCl (A) and $CaCl_2$ (B) concentration at pH 6.0 and 25 ℃.

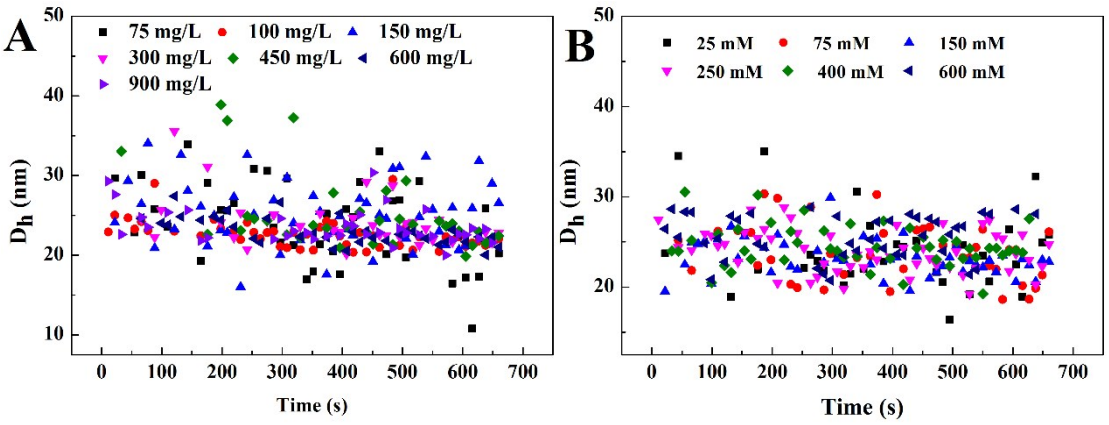

Figure S9. The hydrodynamic diameter (D_h) of OVA at different concentrations in the presence of 120 mM NaCl (A); and the D_h of OVA at 300 mg/L changed as a function of NaCl concentration (B) at pH 6.0 and 25 ℃.

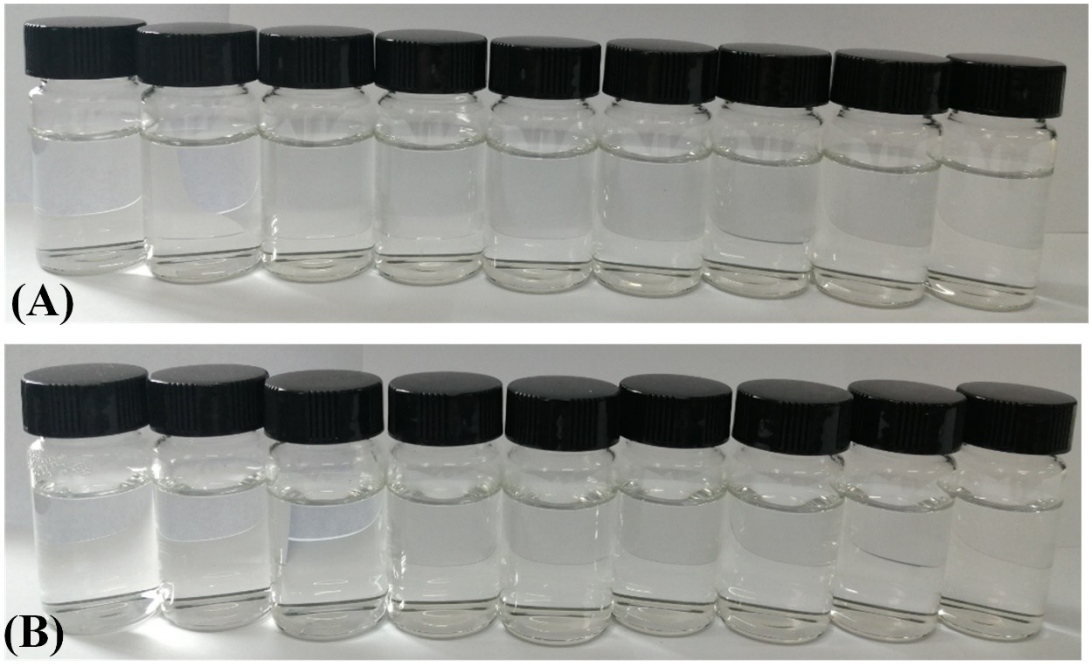

Figure S10. The long-time stability images of BSA at different concentrations (from left to right: 0, 0.5, 1, 2, 5, 10, 20, 50 and 100 mg/L) in the presence of 300 mM NaCl (A) and 10 mM $CaCl_2$ (B) (> CCC values of all GO nanosheets) after 72 h at pH 6.0 and 25 ℃.

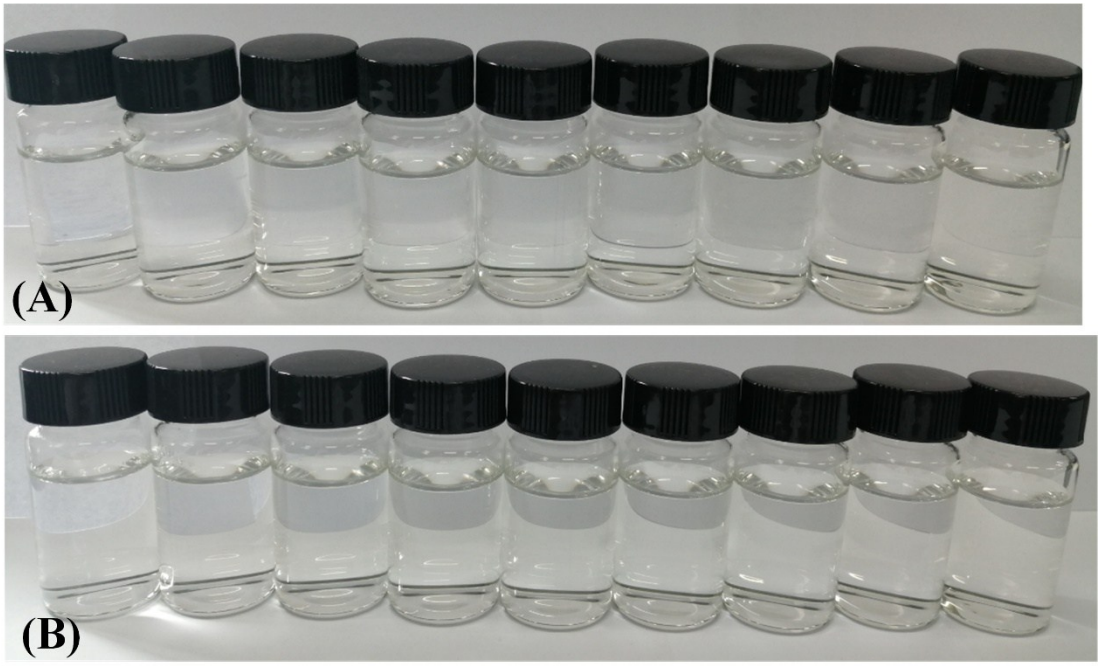

Figure S11. The long-time stability images of OVA at different concentrations (from left to right: 0, 0.5, 2, 5, 10, 50, 100, 300 and 600 mg/L) in the presence of 300 mM NaCl (A) and 10 mM $CaCl_2$ (B) (> CCC values of all GO nanosheets) after 72 h at pH 6.0 and 25 ℃.

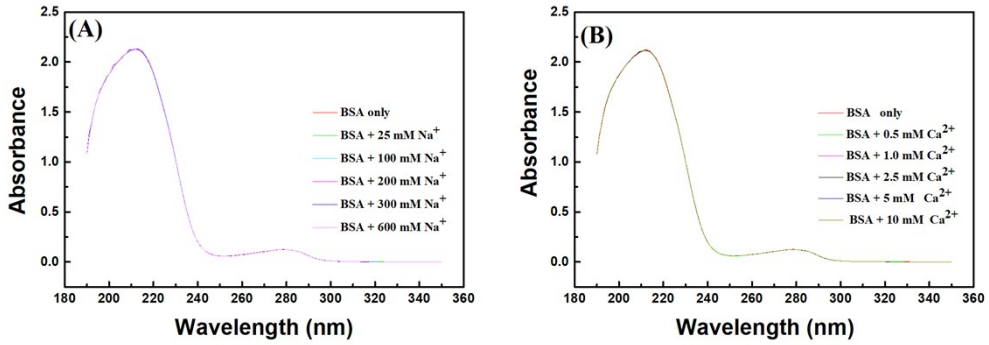

Figure S12. UV-Vis adsorption spectra of BSA (200 mg/L) as a function of (A) NaCl and (B) $CaCl_2$ concentration at pH 6.0 and 25 ℃.

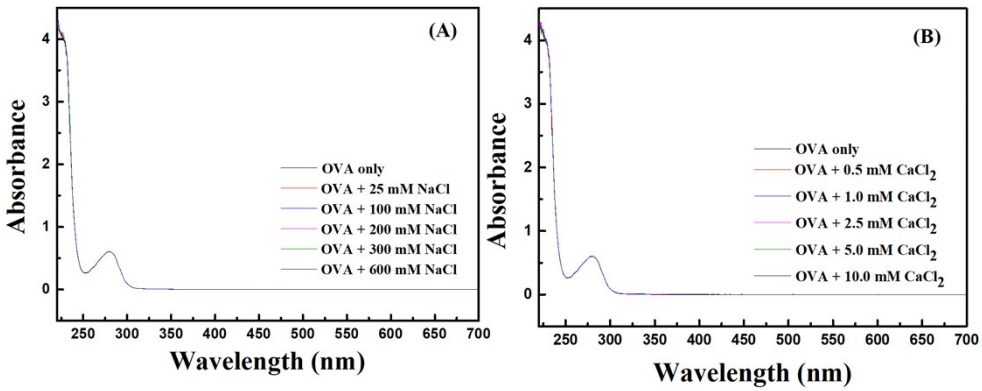

Figure S13. UV-Vis adsorption spectra of OVA (1000 mg/L) as a function of (A) NaCl and (B) $CaCl_2$ concentration at pH 6.0 and 25 ℃.

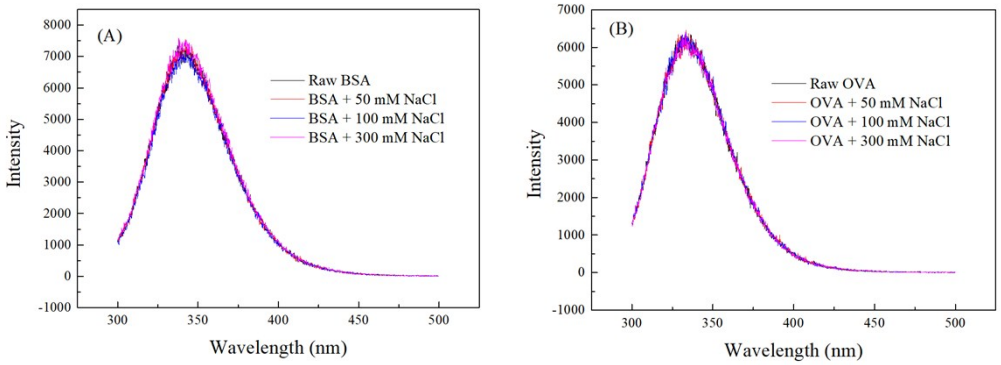

Figure S14. Fluorescence emission spectra of BSA (A) and OVA (B) upon addition of 0-300 mM NaCl. The temperature was set as 25 ℃ and pH 6.0 for all experiments.

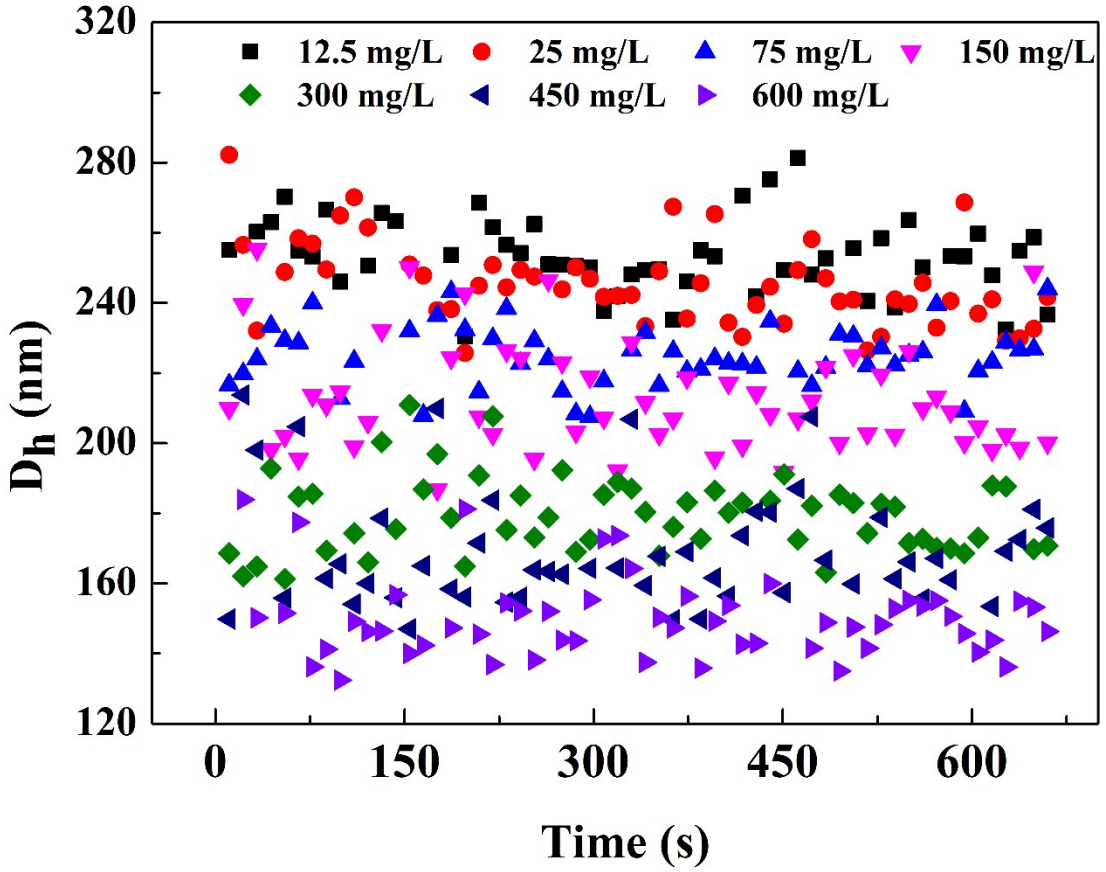

Figure S15. The hydrodynamic diameter (D_h) of 500 nm (GO-2) GO nanoparticles changed as functions of experimental OVA concentration (12.5-600 mg/L) without addition of any salts at pH 6.0 and 25 ℃.

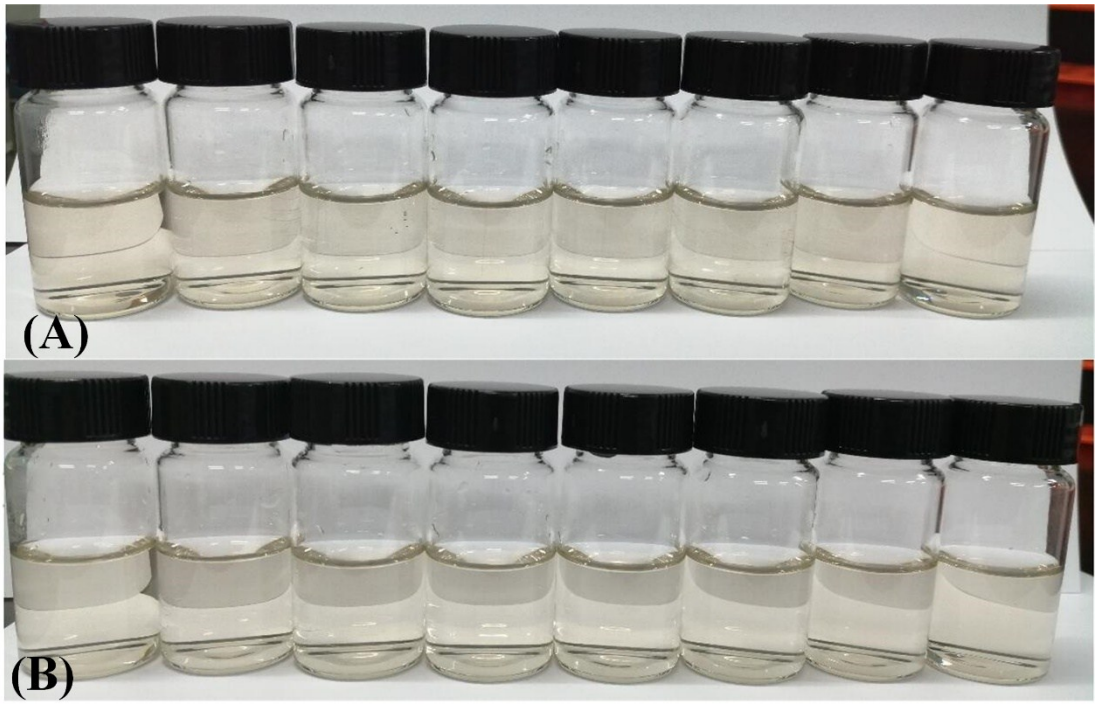

Figure S16. The long-time stability images of GO-2 (10 mg/L) at different protein concentrations without any salts after 72 h at pH 6.0 and 25 ℃. (A) from left to right: 0, 0.5, 2, 5, 10, 50, 100 and 300 mg/L BSA; and (B) 0, 5, 10, 25, 50, 100, 300 and 600 mg/L OVA.

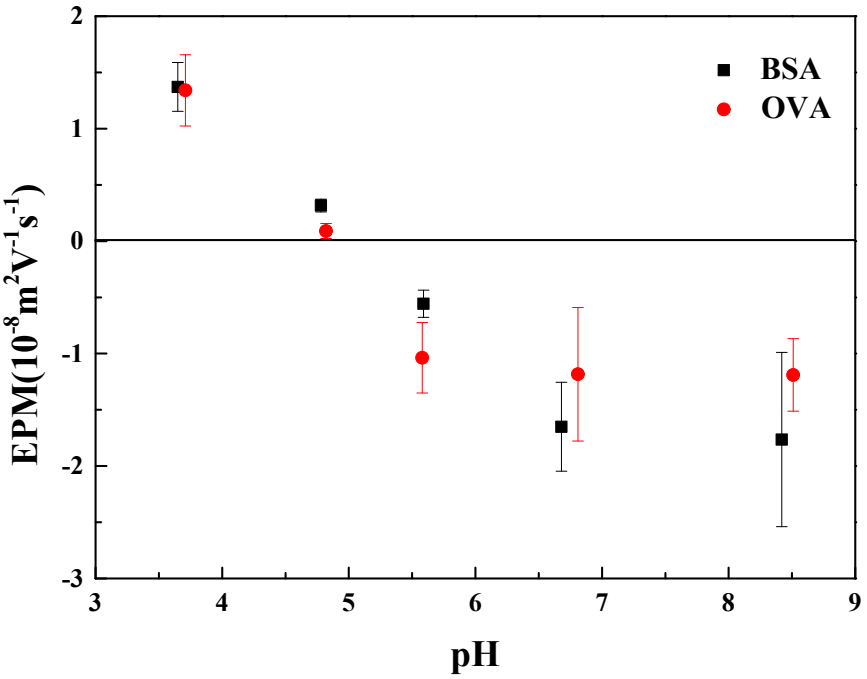

Figure S17. The electrophoretic mobility (EPM) of BSA and OVA (300 mg/L) changed as a function of solution pH at 25 ℃.

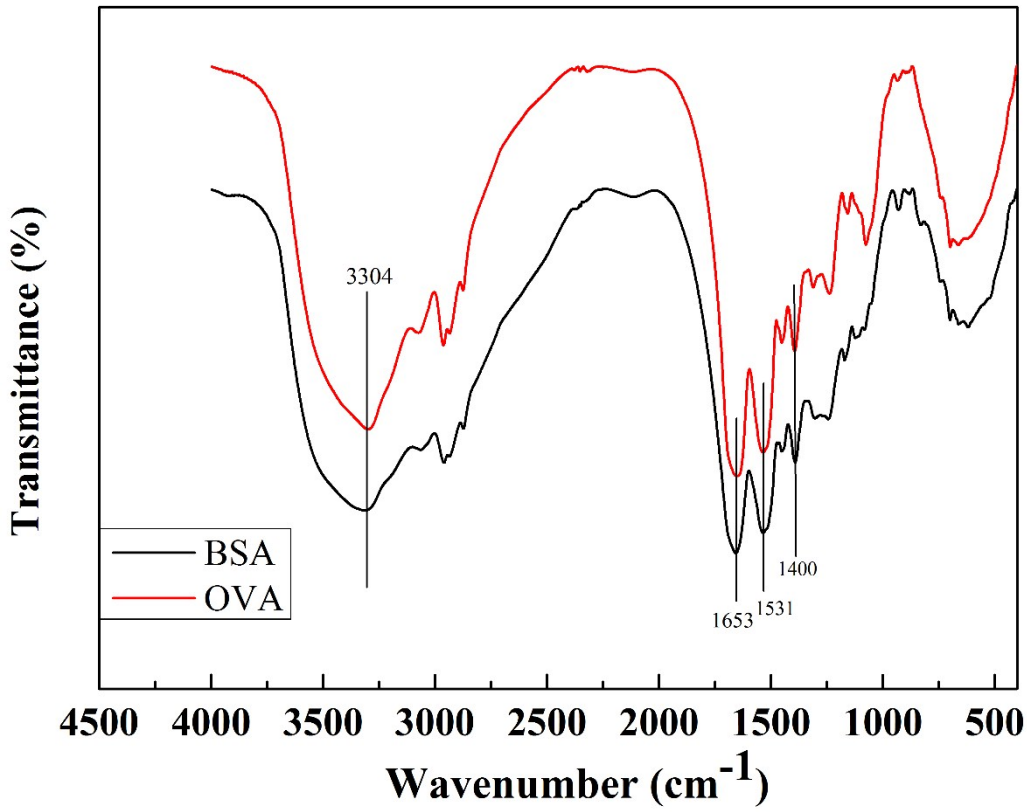

Figure S18. The FTIR spectra of free BSA and OVA powder.

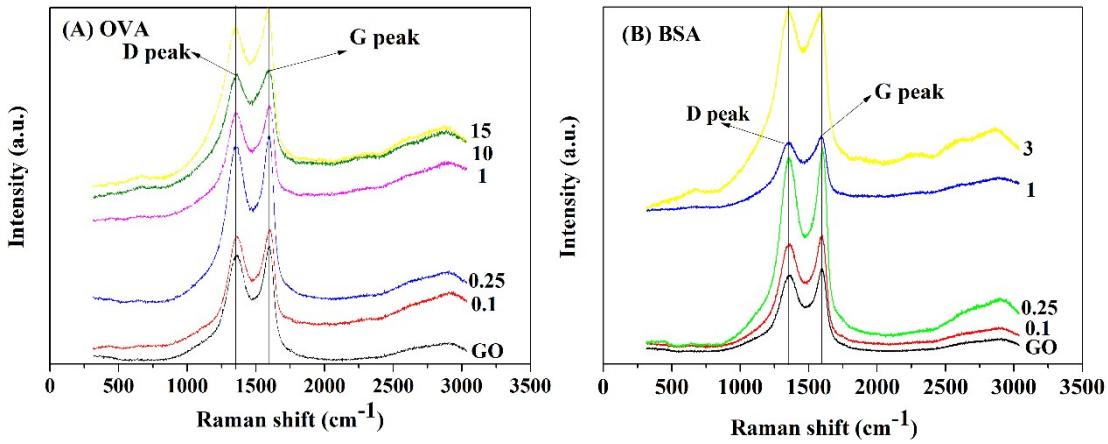

Figure S19. The Raman spectra of GO coated with protein at different protein-to-GO mass ratio (0-15 for OVA-GO complex and 0-3 for BSA-GO complex, respectively).

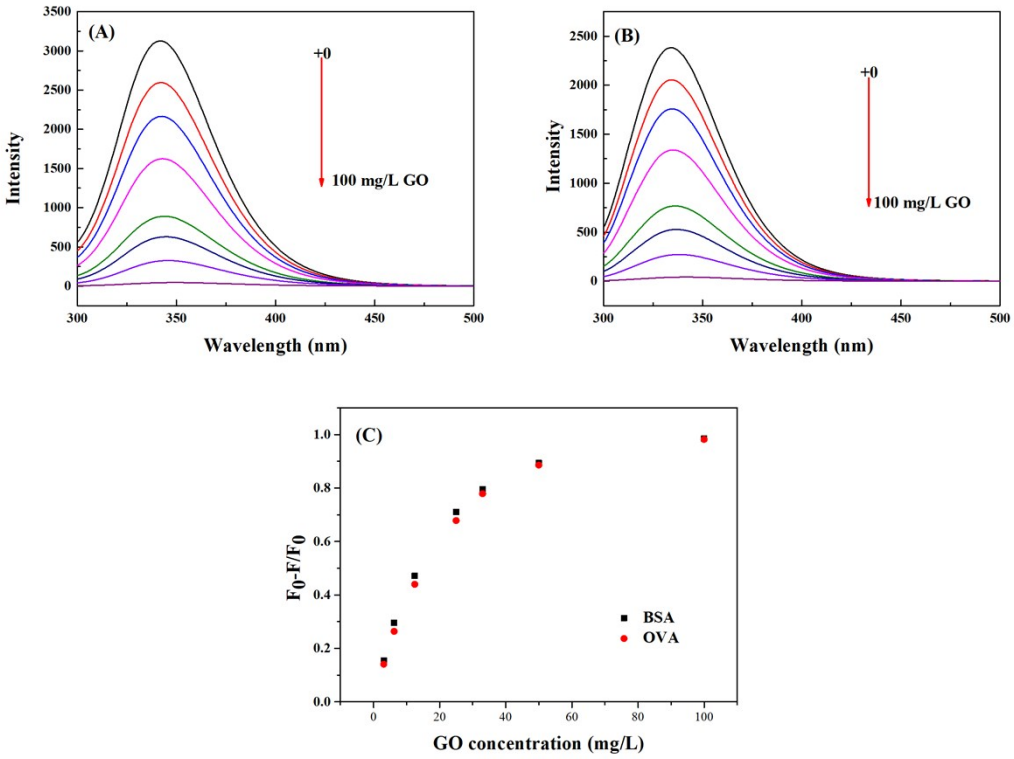

Figure S20. Fluorescence emission spectra of BSA (A) and OVA (B) upon addition of 0-100 mg/L GO. The relationship between normalized fluorescence intensity of BSA and OVA after incubation with GO and the addition of GO concentration (C). All the experiments were conducted at pH 6.0 and 25 ℃.

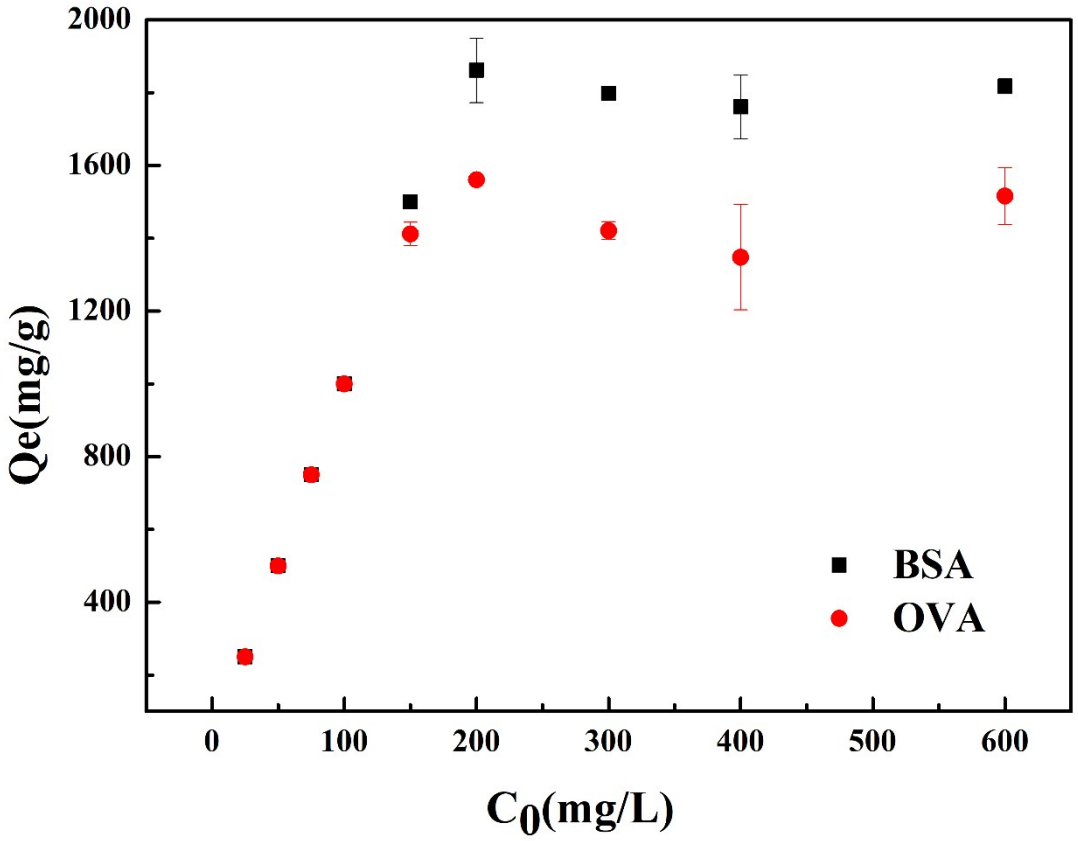

Figure S21. The adsorption isotherms of BSA and OVA at different concentrations on 500 nm (GO-2) GO nanoparticles at pH 6.0 and 25 ℃.

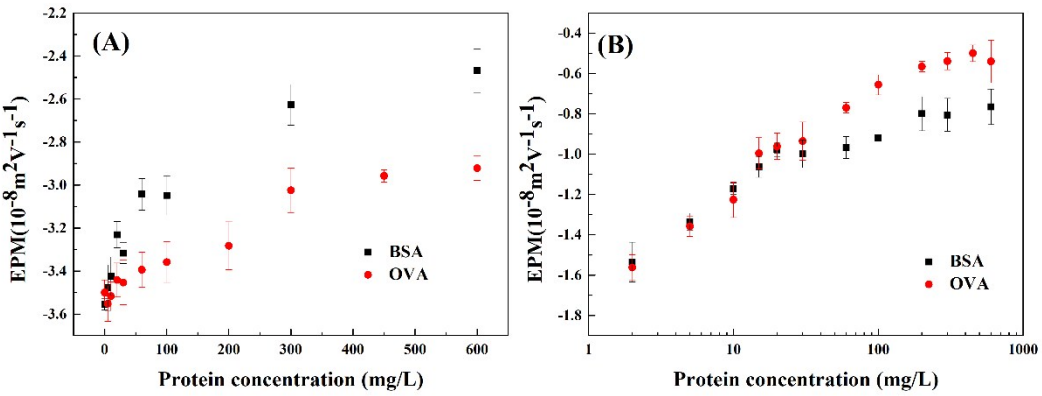

Figure S22. The electrophoretic mobility (EPM) of 500 nm (GO-2) GO nanoparticles changed as functions of protein concentration in the absence of NaCl (A) and presence of 120 mM NaCl (B) at pH 6.0 and 25 ℃.

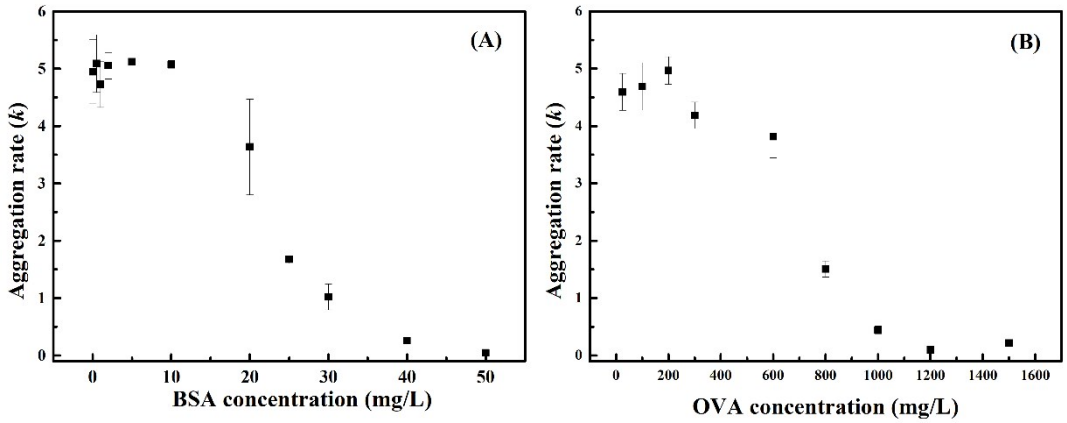

Figure S23. Aggregation rate (k) of 500 nm (GO-2) GO nanoparticles in the presence of BSA (A) and OVA (B) as a function of protein concentration at pH 6.0 and 25 ℃.

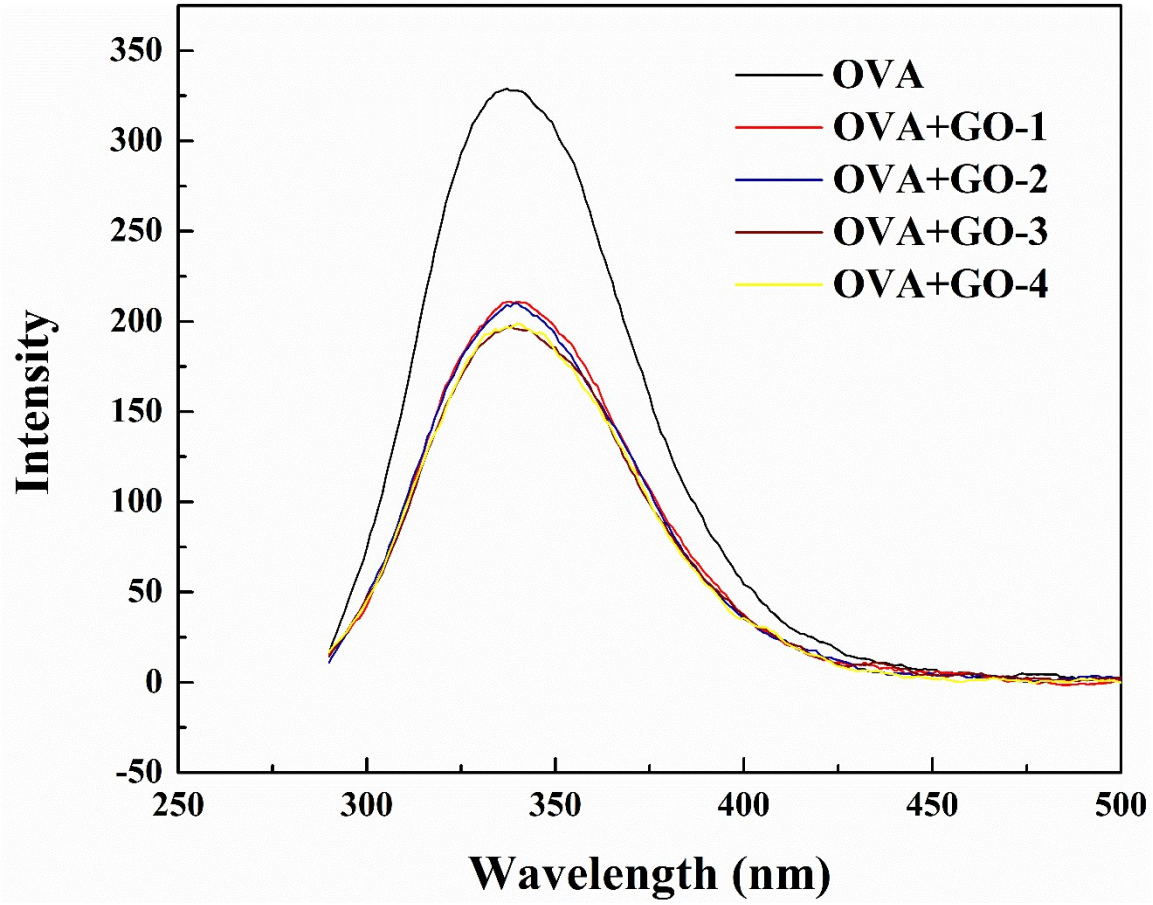

Figure S24. Fluorescence emission spectra of OVA (300 mg/L) after incubated with 1000 nm (GO-1), 500 nm (GO-2), 350 nm (GO-3) and 200 nm (GO-4) GO nanoparticles at pH 6.0 and 25 ℃.

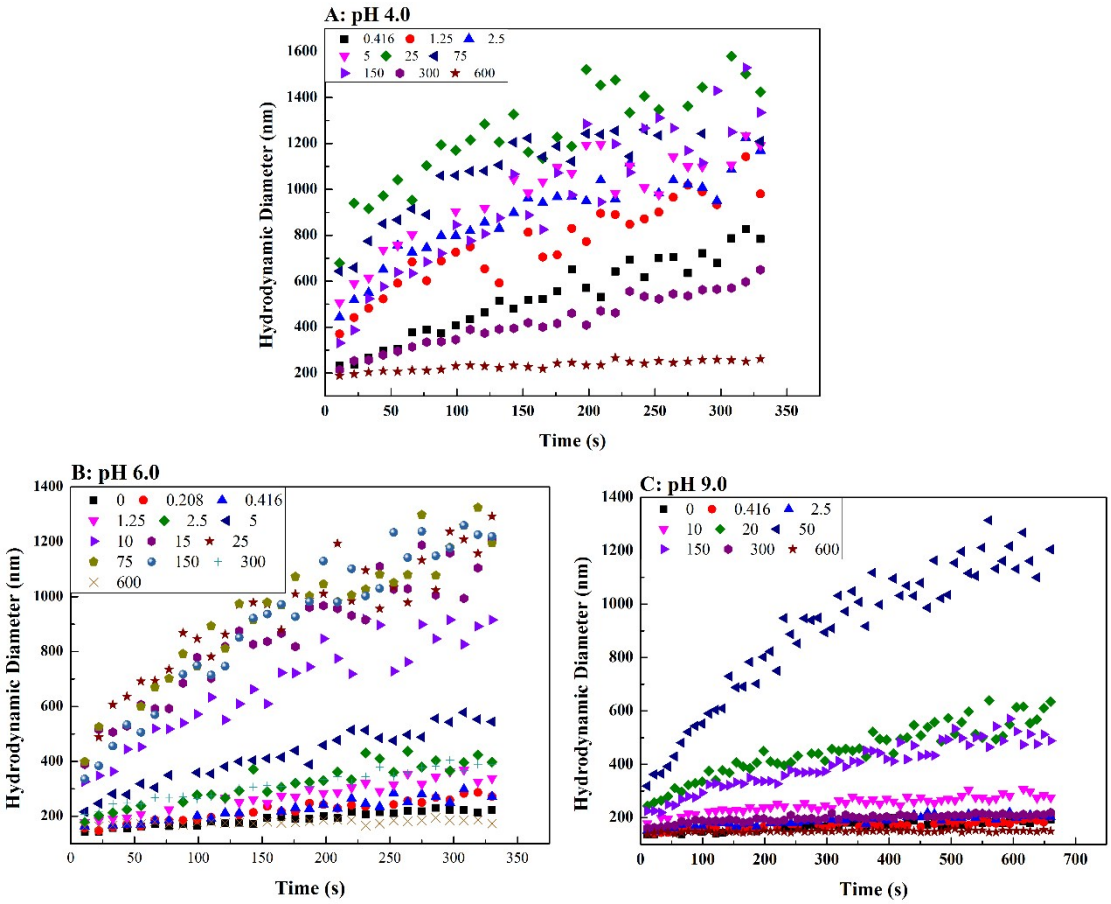

Figure S25. The representative aggregation profiles of 500 nm (GO-2) GO nanoparticles influenced by OVA at different concentrations (0-600 mg/L) under different pH values (4, 6 and 9) at 25 ℃.